

Pressure-Induced Phase Transitions of Hydrous Zirconium Tetrafluoride

HPSTAR
777-2019

Junhua Xi^a and Yanwei Huang^{a, b, *}

^aCollege of Materials and Environmental Engineering, Hangzhou Dianzi University, Hangzhou, 310018 China

^bCenter for High Pressure Science and Technology Advanced Research, Shanghai, 201203 China

*e-mail: ywhuang@hdu.edu.cn

Received June 18, 2018; revised October 10, 2018; accepted December 5, 2018

Abstract—The high pressure behaviors of hydrous zirconium tetrafluoride have been investigated by in situ synchrotron X-ray diffraction, Raman spectroscopy and infrared (IR) absorption measurements. The phase transition occurs under high pressure (0–28 GPa). The α phase transforms into β phase at 7.3 GPa and then γ phase at 13.2 GPa. The high pressure γ phase can be quenched to the starting phase when pressure is releasing to 0 GPa, indicating the reversible phase transition. Furthermore with increasing pressure, fluid molecular water occurs around 11.0 GPa from starting structurally bonded water state according to IR absorption which offer a clue to obtain pure anhydrous salts because of instability of hydrous zirconium tetrafluoride under ambient conditions.

Keywords: hydrous zirconium tetrafluoride, phase transition, high pressure, dehydration

DOI: 10.1134/S1087659619020123

INTRODUCTION

Zirconium tetrafluoride (ZrF_4) is the major constituent of the well-known nonoxide fluorozirconate glasses which are commonly referred to as the heavy-metal fluoride glasses. This heavy metal fluoride belongs to the most remarkable ionic glass which is quite unusual compared to traditional oxide glasses. ZrF_4 has been found to have certain desirable physical and chemical characteristics which make it ideally suitable for a wide variety of applications in optical systems. The glasses based on ZrF_4 have a broad optical transmission window extending into the near IR region and thereby a potential for ultra-low optical losses [1, 2]. They are prime candidates for using as optical-fibers for communications or transmission of optical power to develop IR fiber optic applications. The successful utilization of such fibers hinges on high optical quality in the IR range and superior mechanical properties of the fluorozirconate glass [3]. Besides, ZrF_4 -based materials exhibit the higher conductivities due to fluoride ions, available in the amorphous state. Comprehensively understanding the crystal vibrational properties of ZrF_4 can offer a better knowledge of the anionic conduction mechanism which has a potential application in lithium ion batteries as solid electrolyte.

However, under ambient conditions the presence of the neutral molecule ZrF_4 is rare and it often exists in its hydration state, such as $ZrF_4 \cdot 3H_2O$. If heated, it

cannot transform into pure ZrF_4 without H_2O and it will change into $Zr(OH)_4 \cdot HF$, $ZrO_2 \cdot HF \cdot H_2O$ and $ZrO_2 \cdot ZrF_2 \cdot H_2O$. The behavior of ZrF_4 strongly depends on the intrinsic structure, especially the existence of different ZrF_n ($n = 4-8$) polyhedra presenting a large variety of F–Zr–F bond angles and many possibilities in the local arrangement. The properties are determined by the association of these polyhedra sharing corners or edges. Some works reported improved physical and optical properties of ZrF_4 -based materials by doping Ho^{3+} , Nd^{3+} , and Eu^{3+} cations which act as network modifiers to break the periodicity of the lattice and thereby the external behaviors [4–7]. In practice, introduction of dopant cannot lead stable phase with consideration of size and crystal-chemistry of these cations. The stabilization mechanism should be explored from the existence of polyhedral differing according to their size from ZrF_n polyhedral. It is necessary to develop more progressive techniques to induce structural modifications of ZrF_4 -based materials. The structural modification occurring strongly depends on the materials and the exposure conditions.

Simon Gross et al. [8] reported the femtosecond laser induced structural changes in fluorozirconate glass. They investigated the structural changes within the glass network induced by high repetition rate femtosecond laser pulses and revealed the origin of the observed decrease in refractive index by using Raman

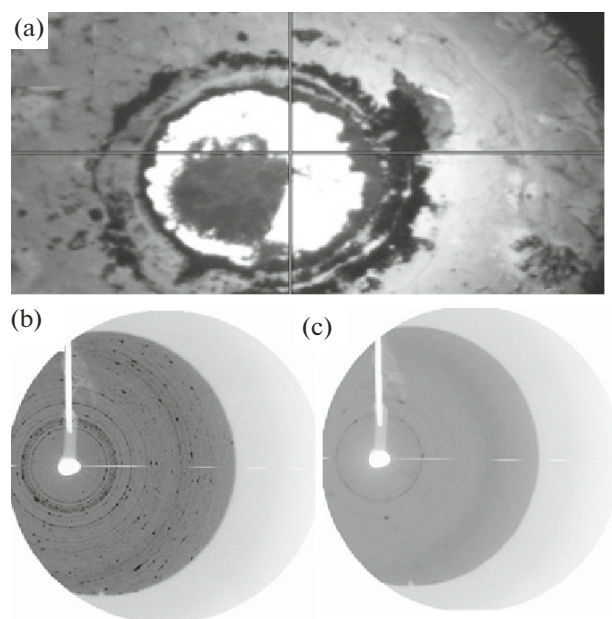


Fig. 1. The hydrous zirconium tetrafluoride loaded in DAC (a) and synchrotron X-ray diffraction rings: (b) 0.5 GPa, (c) 28.0 GPa upon compression.

microscopy. Three crystalline phases of ZrF_4 have been reported, α (monoclinic), β (tetragonal, Pearson symbol tP40, space group $P42/m$, no. 84) and γ phase. β and γ phases are unstable and irreversibly transform into the α phase at 400°C [9]. For a long time the unknown γ - ZrF_4 structure can not be indexed because of the difficulties in synthesis of high-quality single crystals. Recently, with the advanced technique and modern apparatus, Jean-Paul Laval reported the crystal structure of zirconium tetrafluoride, γ - ZrF_4 , under high pressure of 4–8 GPa. The obtained crystal structure is based on the association by corner- and edge-sharing of ZrF_8 triangulated dodecahedra, forming a three-dimensional framework. It presents some analogies with high-temperature α - ZrF_4 but clearly constitutes a new MX_4 structure type [10]. In recent years, pressure can provide a clean way to study the stabilities and the structural transitions of various materials for exploring the potential application in material science [11–15]. However, to the best of our knowledge, there is almost no high pressure studies on hydrous zirconium tetrafluoride ($ZrF_4 \cdot 3H_2O$). It is an interesting research topic for investigating the unique evolution process of $ZrF_4 \cdot 3H_2O$ under high pressure. In this paper, we report the pressure-induced phase transitions of $ZrF_4 \cdot 3H_2O$ using in situ synchrotron X-ray diffraction (XRD), Raman spectroscopy, and IR absorption in diamond anvil cells (DACs) at room temperature.

EXPERIMENTAL

The hydrous zirconium tetrafluoride ($ZrF_4 \cdot 3H_2O$, 99.9%) was purchased from Alfa Aesar without further purification. The X-ray diffraction (XRD) confirmed the triclinic structure at ambient pressure. A symmetric type diamond anvil cell (DAC) with 500 μm diameter culet was used to generate high pressure. $ZrF_4 \cdot 3H_2O$ sample was loaded into a 180 μm diameter hole drilled in T301 stainless steel gasket which was pre-indentated to a thickness of 50 μm . To produce a quasi-hydrostatic environment around the sample, we used silicone oil as a pressure transmitting medium. Pressure was determined by pressure dependent spectral shift of the sharp ruby fluorescence R1 line [16, 17]. The in-situ high pressure XRD experiments were performed at the 15U1 beamline of Shanghai Synchrotron Radiation Facility (SSRF). The incident wavelength of the beam was 0.6199 Å with a beam size of $2 \times 7 \mu m^2$. The high purity CeO_2 powder was used to calibrate the geometric parameters. The FIT2D software was used to integrate the diffraction rings into one-dimensional patterns [18]. The XRD patterns were analyzed with Rietveld refinement using the GSAS program package with a user interface EXP-GUI [19, 20]. In-situ high pressure Raman scattering were performed using a Renishaw inVia Raman spectrometer with excitation wavelength of 532 nm. High pressure infrared absorption measurements were carried out with Hyperion 2000, giving a resolution of 2 cm^{-1} .

RESULTS AND DISCUSSION

Figure 1a shows the well-loaded hydrous zirconium tetrafluoride sample in the DAC for in-situ high pressure synchrotron XRD experiments. Figures 1b and 1c show synchrotron diffraction rings of the starting and compressed sample. As is shown in Fig. 1b, at 0.5 GPa in the process of compression the sample is characterized as powder polycrystalline. The sample at the highest pressure shown in Fig. 1c still maintained its main diffraction peaks but other peaks are very weak and even disappear, which indicating the lattice structure changes with pressure.

Figure 2 shows the pressure evolution of synchrotron XRD patterns for $ZrF_4 \cdot 3H_2O$ upon compression (a) and decompression (b). The diffraction peaks identified in starting structure were consistent with the diffraction planes of triclinic structure (α phase), agreeing with the PDF file no. 70-0583. The weak peak located at 5.5° of 2θ should be due to the existence trace of monohydrate zirconium tetrafluoride ($ZrF_4 \cdot H_2O$). During compression shown in Fig. 2a, the main peaks of (010), (-110), ($0-11$), (-111) and (011) moved to high diffraction angle and became broadened, indicating the reduction of d-spacing or

shrinkage of the unit cells. When the pressure increased to 6.3 GPa, the peak (-110) (marked with $*$) disappeared and the peak $(1-11)$ (marked with $\#$) also disappeared at 7.3 GPa, and meanwhile the new peak appear (marked with β). This indicated the α phase started to transform into the β phase. With further increasing pressure, almost all the peaks of (001) , (010) , (-101) , (-111) , (011) and (101) in the starting structure disappeared due to the complete phase transition. At 13.2 GPa β phase completely transformed to the high pressure γ phase [10]. The weakened intensity of peaks for γ phase implied a low-ordered structure and partial amorphous phase forming. Until the pressure maximum of 28.0 GPa, the γ phase still existed with weakened and broadened peaks, indicating the structure stability. Upon decompression shown in Fig. 2b, when the pressure released to 13.9 GPa, the γ phase started to transform back to β phase, and recovered to α phase at 5.6 GPa. Finally when the pressure released to ambient pressure, the high pressure phase was quenched to the starting phase, which implied the phase transitions were reversible under high pressure.

Raman spectra features are related directly to the vibrational motions of the structural units. Figure 3 shows the Raman spectra of hydrous zirconium tetrafluoride during compression (a) and decompression (b). In Fig. 3a, at 0.9 GPa pressure, there are two Raman active modes observed at 541 and 771 cm^{-1} . The higher frequency mode (541 cm^{-1}) could be assigned to the symmetric stretching vibration of the F–Zr–F bands, which is a common feature from $[\text{ZrF}_n]$ polyhedra as a basic structural units. And the weak peak locating at 771 cm^{-1} was due to pressure transmitting medium: silicone oil, which has been confirmed with other pressure transmitting medium [21–23]. With the pressure increasing, the Raman peak 541 cm^{-1} weakened with blueshift, and disappeared at 13.8 GPa. When the pressure achieved 20.8 GPa, The Raman signal can not be detected further. This is basically consistent with the results of XRD in which the two phase transition processes appeared. Upon decompression, in Fig. 3b the intensity of the Raman peak turns obvious until the pressure is released to 14.6 GPa. When the pressure is released to 0.2 GPa, the high pressure phase almost completely transformed back into the starting phase, which revealed the sample has reversible phase transition under high pressure. This phase transition has been conformed by the results of synchrotron XRD.

The high pressure IR spectra of hydrous zirconium tetrafluoride are shown in Fig. 4. The bands in the region 600–750 cm^{-1} are zirconium-fluorine stretching modes which are not obvious because of the intensity of hydrous compounds bands [24]. The broad absorption peaks observed at around 3300 cm^{-1} are in the range of the OH-stretching vibration and those

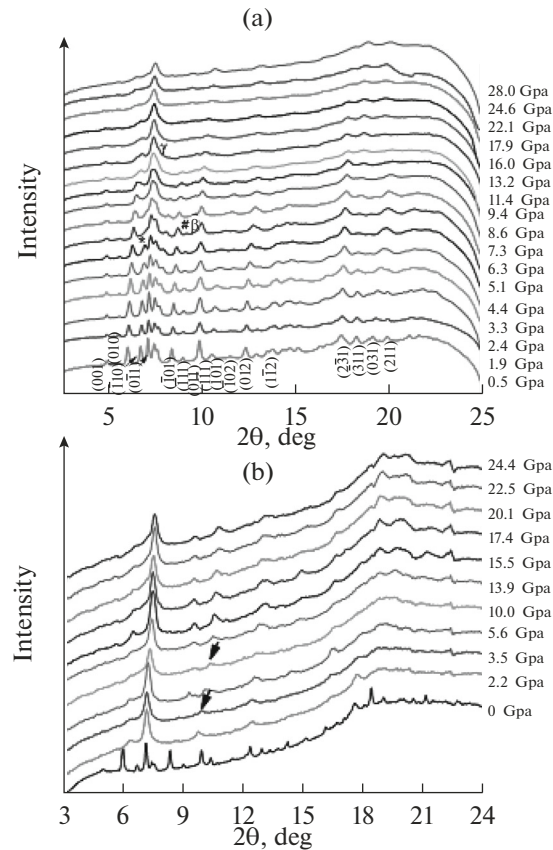


Fig. 2. Synchrotron XRD patterns of hydrous zirconium tetrafluoride under high pressure. (a) Compression; (b) decompression.

observed at 1600 cm^{-1} are assumed to be caused by the HOH-bending vibration mode [25, 26]. Kagi et al. [27] argued the vibration mode locating at 1600 cm^{-1} should be attributed to the molecular water occurring both as fluid inclusions and/or as structurally bound molecular water in their hydrous ringwoodite ($\gamma\text{-Mg}_2\text{SiO}_4$) samples. For hydrous zirconium tetrafluoride, upon compression shown in Fig. 4a the band of 1600 cm^{-1} should be ascribed to the structurally bound molecular water at starting state. With increasing pressure, the peak intensity of 1600 cm^{-1} turns weak or even blurry above 11.0 GPa which reveals more fluid molecular water occurs. This means pressure can induce $\text{ZrF}_4 \cdot 3\text{H}_2\text{O}$ losing part molecular water while maintain the chemical composition of ZrF_4 which is different under ambient conditions. Thus pressure can be a method to obtain pure anhydrous salts. The broad band around 3300 cm^{-1} always exist upon compression because the OH-stretching vibration exist all through the hydrous or anhydrous zirconium tetrafluoride. As shown in Fig. 4b, upon decompression when the pressure is releasing to ambient pressure the IR spectrum agrees with the starting state which indicates the process is

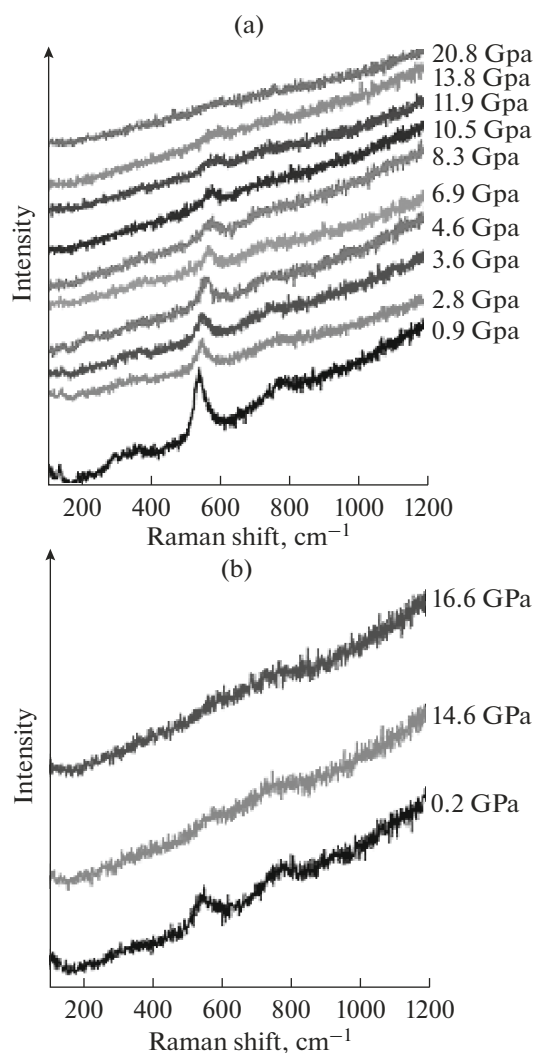


Fig. 3. In situ high pressure Raman spectra at various pressures: (a) compression; (b) decompression.

reversible. This is consistent with the results of synchrotron XRD and Raman which reveal phase transitions were reversible under high pressure.

CONCLUSIONS

The high pressure-induced phase transitions were studied by in situ synchrotron radiation, Raman spectroscopy, IR absorption in hydrous zirconium tetrafluoride as starting material. The XRD results revealed the phase transition from α phase to β phase and then to γ phase in the process of compression to 28 GPa. In the process of decompression the high pressure γ phase can be quenched to the starting phase, indicating the reversible phase transition. The form of molecular water in hydrous zirconium tetrafluoride under high pressure has been discussed according to IR absorption measurement. Upon compression free molecular water can be dissociated from the $ZrF_4 \cdot$

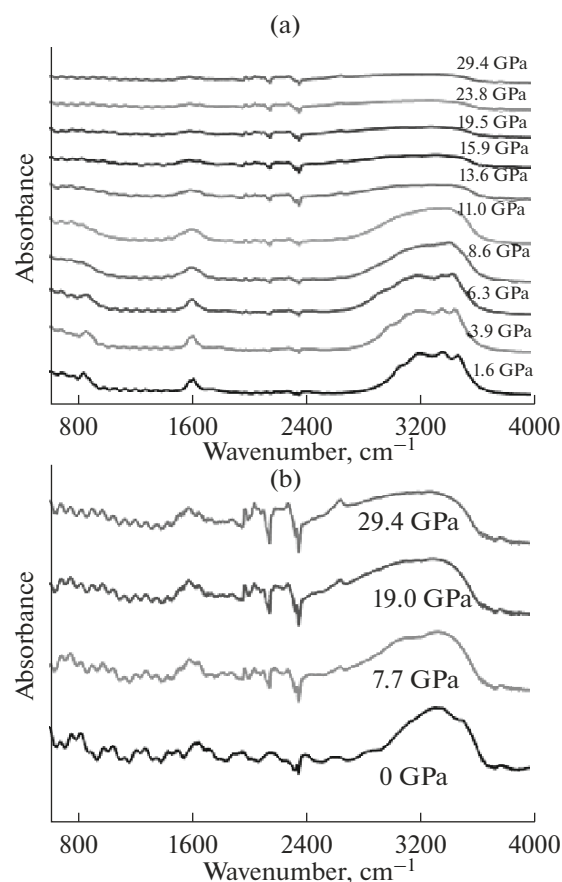


Fig. 4. Infrared spectrum of hydrous zirconium tetrafluoride at high pressure: (a) compression; (b) decompression.

$3H_2O$ which offer us a method to obtain the anhydrous salts from their hydrates. These high pressure behaviors about hydrous zirconium tetrafluoride provide reference for a series of nonoxide fluorozirconate glasses.

FUNDING

This work was supported by Natural Science Foundation of China (Grant no. 61504034) and Science and Technology Project of Zhejiang Province (no. 2015C37037).

REFERENCES

1. Aasland, S., Einarsrud, M.-A., Grande, T., Grzechnik, A., and McMillan, P.F., The structure of ternary fluorozirconate glasses, *J. Non-Cryst. Solids*, 1997, vols. 213–214, pp. 341–344. doi 10.1016/S0022-3093(97)00070-7
2. Adichtchev, S.V., Malinovsky, V.K., Ignatieva, L.N., Merkulov, E.B., and Surovtsev, N.V., Low-frequency inelastic light scattering in a ZBLAN (ZrF_4 – BaF_2 – LaF_3 – AlF_3 – NaF) glass, *J. Chem. Phys.*, 2014, vol. 140, p. 184508. doi 10.1063/1.4875095

3. Drexhage, M.G., Ei-Bayoumi, O.H., Lipson, H., Moynihan, C.T., Bruce, A.J., Lucas, J., and Fonteneau, G., Comparative study of BaF₂/ThF₄ glasses containing YF₃, YbF₃ and LuF₃, *J. Non-Cryst. Solids*, 1983, Vol. 56, nos. 1–3, pp. 51–56. doi 10.1016/0022-3093(83)90445-3
4. Amaranath, G., Buddhudu, S., and Bryant, F.J., Spectroscopic properties of Tb³⁺-doped fluoride glasses, *J. Non-Cryst. Solids*, 1990, vol. 122, no. 1, pp. 66–73. doi 10.1016/0022-3093(90)90226-C
5. Hanumanthu, M., Annapurna, K., and Buddhudu, S., Fluorescence characteristics of Nd³⁺-doped heavy metal fluoride glasses, *Solid State Commun.*, 1991, vol. 80, no. 5, pp. 315–320. doi 10.1016/0038-1098(91)90137-K
6. Annapurna, K. and Buddhudu, Fluorescence properties of Eu³⁺-doped ZrF₄ based optical glasses, *Phys. J. D: Appl. Phys.*, 1993, vol. 26, pp. 302–306.
7. Lipinska-Kalita, K.E., Auzel, F., and Santa-Cruz, P., Raman and spectroscopic studies of the early steps of crystallization in ZrF₄–LaF₃–AlF₃–ErF₃ glass, *J. Non-Cryst. Solids*, 1996, vol. 204, pp. 188–195. doi 10.1016/S0022-3093(96)00408-5
8. Gross, S., Lancaster, D.G., Ebendorff-Heidepriem, H., et al., Femtosecond laser induced structural changes in fluorozirconate glass, *Opt. Mater. Express*, 2013, vol. 3, no. 5, pp. 574–583. doi 10.1364/OME.3.000574
9. Brown, P.L., Mompean, F.J., Perrone, J., and Illemassène, M., *Chemical Thermodynamics of Zirconium*, Amsterdam: Gulf Professional, 2005, p. 144.
10. Laval, J.-P., Crystal chemistry of anion-excess ReO₃-related phases. γ -ZrF₄, a high-pressure form of zirconium tetrafluoride, and a comparison of MX₄ structure types, *Acta Crystallogr., Ser. C*, 2014, vol. 70, pp. 742–748. doi 10.1107/S2053229614014338
11. Hitosugi, T., Yamada, N., Nakao, Sh., Hirose, Y., and Hasegawa, T., Properties of TiO₂-based transparent conducting oxides, *Phys. Status Solidi A*, 2010, vol. 207, pp. 1529–1537. doi 10.1002/pssa.200983774
12. Nishi, M., Irifune, T., Tsuchiya, J., Tange, Y., Nishihara, Y., Fujino, K., Higo, Y., Stability of hydrous silicate at high pressures and water transport to the deep lower mantle, *Nat. Geosci.*, 2014, vol. 7, pp. 224–227. doi 10.1038/ngeo2074
13. Huang, Y., Chen, F., Li, X., et al., Pressure-induced phase transitions of exposed curved surface nano-TiO₂ with high photocatalytic activity, *J. Appl. Phys.*, 2016, vol. 119, p. 215903. doi 10.1063/1.4953218
14. Huang, Y., Li, W., Ren, X., Yu, Zh., Samanta, S., Yan, Sh., Zhang, J., and Wang, L., *Radiat. Phys. Chem.*, 2016, vol. 120, pp. 1–6. doi 10.1016/j.radphyschem.2015.11.008
15. Hong, F., Yue, B., Hirao, N., Liu, Zh., and Chen, B., Significant improvement in Mn₂O₃ transition metal oxide electrical conductivity via high pressure, *Sci. Rep.*, 2017, vol. 7, p. 44078. doi 10.1038/srep44078
16. Dylla, A.G., Henkelman, G., and Stevenson, K.J., Lithium insertion in nanostructured TiO₂(B) architectures, *Acc. Chem. Res.*, 2013, vol. 46, pp. 1104–1112. doi 10.1021/ar300176y
17. Zhang, J., Xi, J., and Ji, Z., Mo+N codoped TiO₂ sheets with dominant {001} facets for enhancing visible-light photocatalytic activity, *J. Mater. Chem.*, 2012, vol. 22, p. 17700. doi 10.1039/C2JM32391E
18. Hammersley, A.P., Svensson, S., Hanfland, M., Fitch, A.N., and Hausermann, D., Two-dimensional detector software: From real detector to idealised image or two-theta scan, *High Press. Res.*, 1996, vol. 14, nos. 4–6, pp. 235–248. doi 10.1080/08957959608201408
19. Larson, A.C. and von Dreele, R.B., Los Alamos National Laboratory Report LAUR 86-748, 2004.
20. Toby, B.H., EXPGUI, a graphical user interface for GSAS, *J. Appl. Crystallogr.*, 2001, vol. 34, pp. 210–213. doi 10.1107/s0021889801002242
21. Walrafen, G.E., Hokmabi, M.S., Guha, S., and Krishnan, P.N., Low-frequency Raman investigation of lead-containing fluorozirconate glasses and melts, *J. Chem. Phys.*, 1985, vol. 83, p. 4427. doi 10.1063/1.449061
22. Dracopoulos, V., Vagelatos, J., and Papatheodorou, G.N., Raman spectroscopic studies of molten ZrF₄-KF mixtures and of A₂ZrF₆, A₃ZrF₇ (A = Li, K or Cs) compounds, *J. Chem. Soc., Dalton Trans.*, 2001, pp. 1117–1122. doi 10.1039/B008433F
23. Almeida, R.M. and Mackenzie, J.D., Vibrational spectra and structure of fluorozirconate glasses, *J. Chem. Phys.*, 1981, vol. 74, pp. 5954–5961. doi 10.1016/0022-3093(82)90005-9
24. Coombes, J.S. and Spaziant, P.M., The infrared spectrum (4000–33 cm⁻¹) of niobium tetrafluoride compared with other metal tetrafluorides, *J. Inorg. Nucl. Chem.*, 1969, vol. 31, pp. 2636–2638. doi 10.1016/0022-1902(69)80606-8
25. Ohtani, E., Mizobata, H., and Yurimoto, H., Stability of dense hydrous magnesium silicate phases in the systems Mg₂SiO₄-H₂O and MgSiO₃-H₂O at pressures up to 27 GPa, *Phys. Chem. Minerals*, 2000, vol. 27, pp. 533–544. doi 10.1007/s002690000097
26. Kanzaki, M., Stability of hydrous magnesium silicates in the mantle transition zone, *Phys Earth Planet Inter.*, 1991, vol. 66, pp. 307–312. doi 10.1016/0031-9201(91)90085-V
27. Kagi, H., Inoue, T., Weidner, D.J., Lu, R., and Rossman, G.R., Speciation of hydroxides in hydrous phase synthesized at high pressure and temperature, in *Proceedings of the Japanese Earth Planet Science Joint Meeting*, 1997, p. 506.